JETIR.ORG ISSN: 2349-5162 | ESTD Year : 2014 | Monthly Issue
JOURNAL OF EMERGING TECHNOLOGIES AND INNOVATIVE RESEARCH (JETIR)
An International Scholarly Open Access, Peer-reviewed, Refereed Journal

Comparative Study of Edge- Preserving Smoothing Bilateral Filter

Sourav Dutta
Student of M.tech (ECE)

Arpita Santra
Assistant Professor

Sangita Roy
Associate Professor

Electronic and Communications Engineering Department
Narula Institute of Technology, Agarpara, Kolkata

ABSTRACT:Edge-Preserving Smoothing is a very important operator in the image processing as well as in computer vision section. It's an image processing technique that smooth's away noise or textures while retaining sharp edges. Bilateral filter smooth's an input image while preserving edges, by means of a non-linear combination of image values. It replaces the intensity of each pixel with a weighted average of its neighbours. Each neighbour is weighted by a spatial component that penalizes distant pixels and range component that penalizes pixels with a different intensity. Bilateral filter parameters are: SSIM, PSNR, NIQE. The bilateral filter gradually approaches Gaussian convolution more closely because the range Gaussian widens and flattens, which means that it becomes nearly constant over the intensity interval of the image. As the spatial parameters increases, the larger features get smoothened.

Key words- Bilateral image filter, edge- preserving, smoothening filter, simultaneous, parameters.

1. INTRODUCTION

The bilateral filter is a non-linear technique that can blur an image while respecting strong edges. Its ability to decompose an image into different scales without causing haloes after modification has made it ubiquitous in computational photography applications such as tone mapping, style transfer, relighting, and denoising. This text provides a graphical, intuitive introduction to bilateral filtering, a practical guide for efficient implementation and an overview of its numerous applications, as well as mathematical analysis. It can be traced back to 1995 with the work of Aurich and Weule [1995] on nonlinear Gaussian filters. It has been later rediscovered by Smith and Brady [1997b] as part of their SUSAN framework, and Tomasi and Manduchi [1998] who gave it its current name. Since then, the use of bilateral filtering has grown rapidly and is now ubiquitous in image-processing applications.

1.1 IMAGE SMOOTHING WITH GAUSSIAN CONVOLUTION

In image processing, a **Gaussian blur** (also known as **Gaussian smoothing**) is a two- dimensional operator that is used to 'blur' images and remove detail and noise. In this sense it is similar to the mean filter, but it uses a different kernel that represents the shape of a Gaussian ('bell-shaped') hump.

It is a widely used effect in graphics software, typically to reduce image noise and reduce detail. The visual effect of this blurring technique is a smooth blur resembling that of viewing the image through a translucent screen, distinctly different from the bokeh effect produced by an out-of-focus lens or the shadow of an object under usual illumination.

Gaussian smoothing is also used as a pre-processing stage in electronic, computer vision algorithms in order to enhance image structures at different scales—see scale space representation and scale space implementation.

1.2 EDGE-PRESERVING FILTER WITH THE BILATERAL FILTER

The bilateral filter is also defined as a weighted average of nearby pixels, in a manner very similar to Gaussian convolution. The difference is that the bilateral filter takes into account the difference in value with the neighbours to preserve edges while smoothing. The key idea of the bilateral filter is that for a pixel to influence another pixel, it should not only occupy a nearby location but also have a similar value. It is uses of a variety of applications are: Denoising, Texture and Illumination Separation, Data Fusion, 3D Fairing, and other.

2. METHOD

The method of bilateral filter is defined following-

$$I^{\text{filtered}}(x) = \frac{1}{W_p}\sum_{x_i\in\Omega} I(x_i) f_r(\|I(x_i) - I(x)\|) g_s(\|x_i - x\|) \quad (1)$$

And normalization term Wp, is defined as

$$W_p = \sum_{x_i\in\Omega} f_r(\|I(x_i) - I(x)\|) g_s(\|x_i - x\|) \quad (2)$$

Where

I^{filtered} = Is the filtered image.
I = Is the original input image to be filtered.
x = Are the coordinates of the current pixel to be filtered
Ω = Is the window centered in , so is another pixel;
f_r = Is the range kernel for smoothing differences in intensities.
g_s = Is the spatial (or domain) kernel for smoothing differences in coordinates (this function can be a Gaussian function).

The weight W_p is assigned the spatial closeness and the intensity difference Consider a pixel located in k, l that needs to be denoised in image using its neighbouring pixels and located one of its neighboring pixels is k, l . Then, the range and spatial kernels to be Gaussian kernels, the weight assigned for pixel denoted as k, l to denoise the pixel i, j is

$$w(i,j,k,l) = \exp\left(-\frac{(i-k)^2+(j-l)^2}{2\sigma_d^2} - \frac{\|I(i,j)-I(k,l)\|^2}{2\sigma_r^2}\right) \quad (3)$$

Where σ_d and σ_r are smoothing, and $I(i, j)$ and $I(k, l)$ are the intensity of pixels i, j and k, l respectively.

After the weights calculating, normalize:-

$$I_D(i,j) = \frac{\sum_{k,l} I(k,l) w(i,j,k,l)}{\sum_{k,l} w(i,j,k,l)} \quad (4)$$

3. RESULT ANALYSIS

We experimented with the BLF by changing both the regularization parameter (ϵ) and the radius of the square window (r) on different sets of images. Each set consists of two types of result analysis they are: smoothing of image, SSIM, PSNR, NIQE analysis.

TABLE 1

Comparison with different parameter in different Gray scale images

Input Image Name	Size	Type	Degree of Smoothing	SSIM	PSNR	NIQE (I) (J)
Eagle.jpg	900x600x3	uint8	289.6081	0.9907	44.5494	(i)2.5368 (j)2.8843
Bird.jpg	1063x1600x3	uint8	490.7766	0.9751	43.1513	(i)2.4384 (j)4.1333
Fish.jpg	600x548x3	uint8	13.2572	0.9994	59.6488	(i)3.7585 (j)4.2999
Flower.jpg	566x736x3	uint8	6388.063	0.9856	41.7023	(i)3.2436 (j)4.4636
Cat.jpg	900x600x3	uint8	365.2348	0.9874	43.3868	(i)7.8831 (j)6.0211

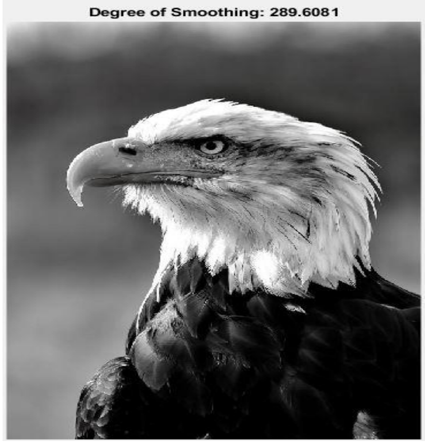

Fig 1. (a) input image of eagle.jpg (b) output image of eagel.jpg in bilateral filter

Fig 2 (a) input image of bird.jpg (b) output image of bird.jpg in bilateral filter

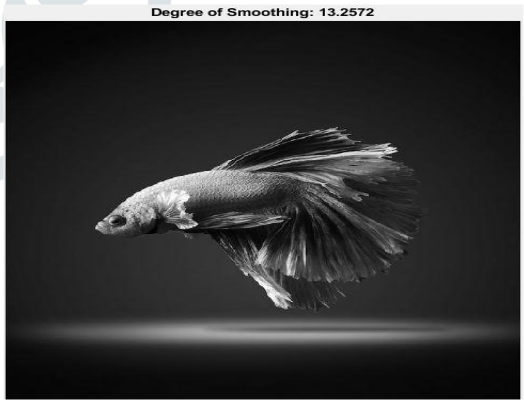

Fig 3 **a**) input image of fish.jpg (b) output image of fish.jpg in bilateral filter

Fig 4 a) input image of flower.jpg (b) output image of flower.jpg in bilateral filter

Fig 5 a) input image of cat.jpg

(b) output image of cat.jpg in bilateral filter

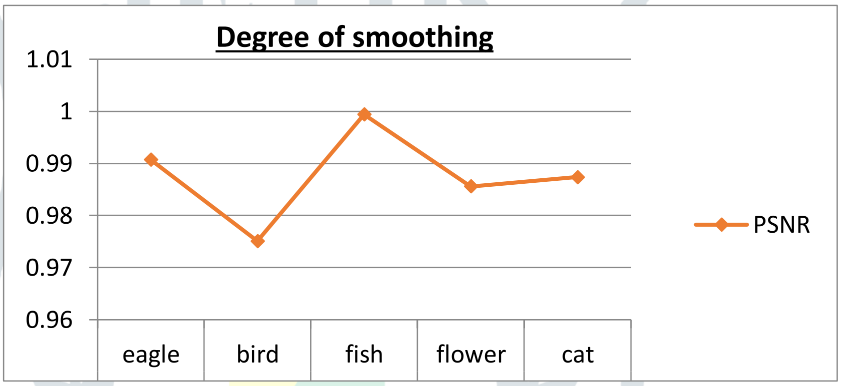

Fig 6. Experimental data of images with Degree of smoothing graph.

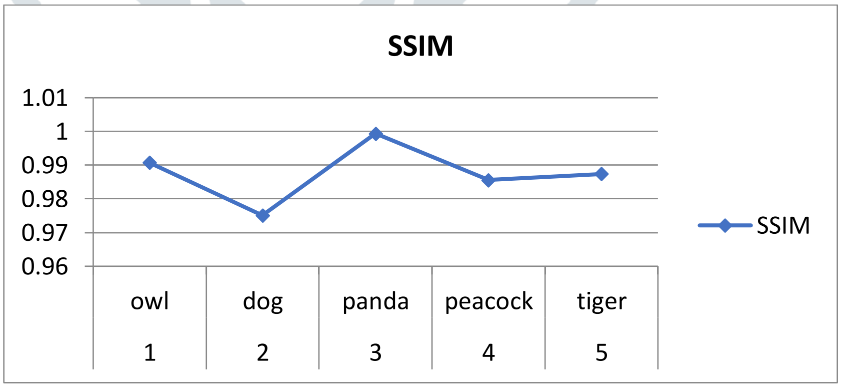

Fig 7. Experimental data of images with SSIM (Structural Similarity Index Measure) graph.

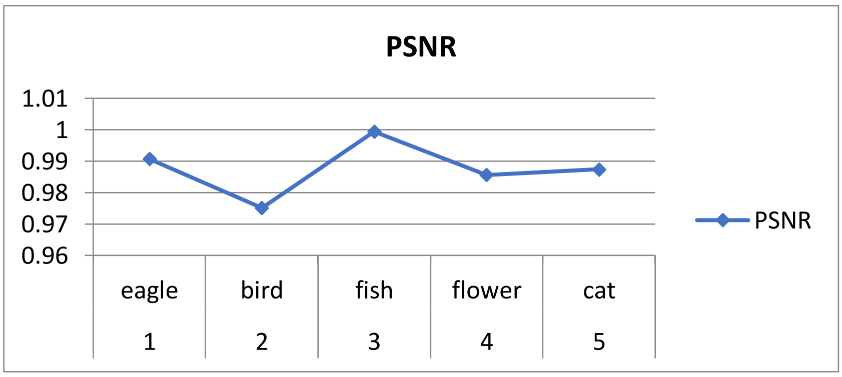

Fig 8. Experimental data of images with PSNR (Peak Signal-to-Noise Ratio) graph.

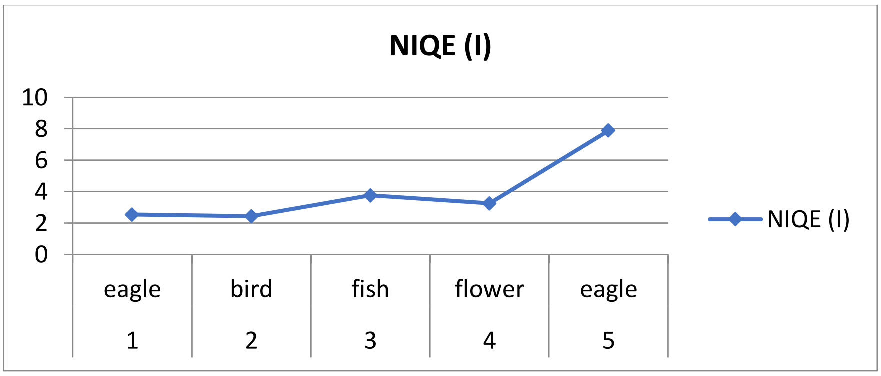

Fig 9. Experimental data of images with Naturalness Image Quality Evaluator (NIQE (I)) graph.

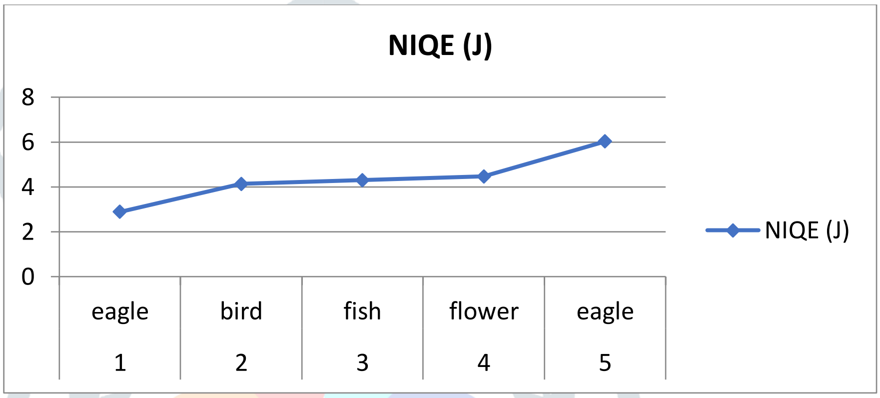

Fig10. Experimental data of images with Naturalness Image Quality Evaluator (NIQE (J)) graph.

TABLE-2

Comparison with different parameter in different RGB scale images.

Input Image Name	Size	Type	Degree of Smoothing	SSIM	PSNR	NIQE (I) (J)
Owl	768X 1024X3	double	903.7545	0.9853	37.5717	(I)2.5744 (j)2.9692
Dog	2050x3072x3	uint8	3719.2067	0.9859	33.1948	(I)2.8371 (j)3.6723
Panda	2050x3072x3	uint8	1336.0145	0.9738	38.7736	(i)2.3216 (j)2.7878
Peacock	2050x3072x3	uint8	2192.3064	0.9859	33.8065	(i)2.7216 (j)3.2790
Tiger	300x498x3	uint8	4831.422	0.9853	32.4866	(i)3.2770 (j)4.2035

Fig 11 a) input image of owl.jpg

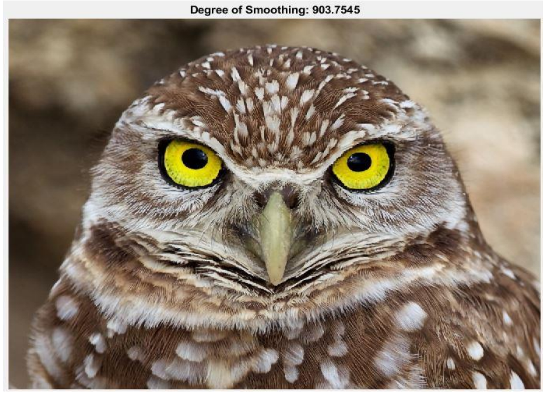

(b) output image of eagel.jpg in bilateral filter

Fig 12 a) input image of dog.jpg

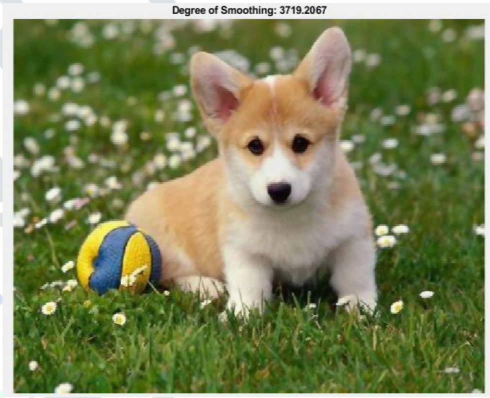

(b) output image of dog.jpg in bilateral filter

Fig 13 a) input image of panda.jpg

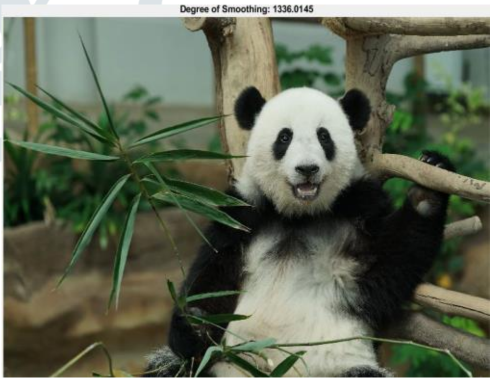

(b) output image of panda.jpg in bilateral filter

Fig 14 a) input image of peacock.jpg

(b) output image of peacock.jpg in bilateral filter

Fig 15 a) input image of tiger.jpg

(b) output image of tiger.jpg in bilateral filter

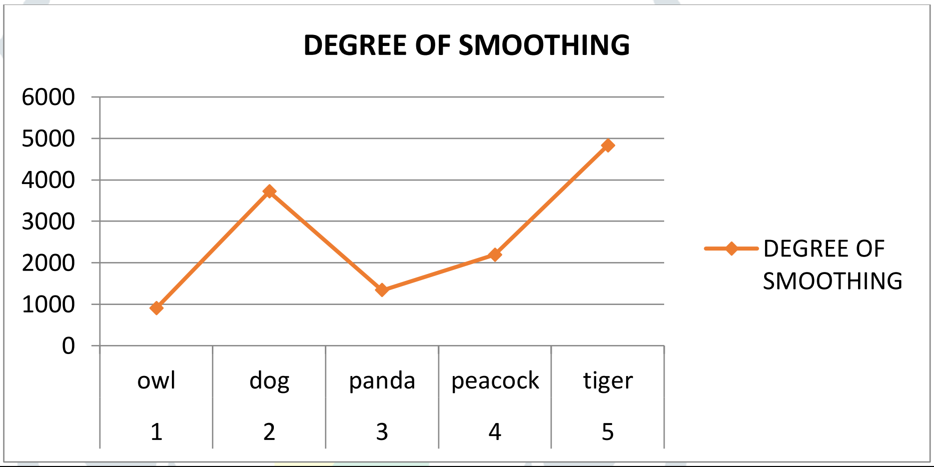

Fig 16. Experimental data of images with Degree of smoothing graph.

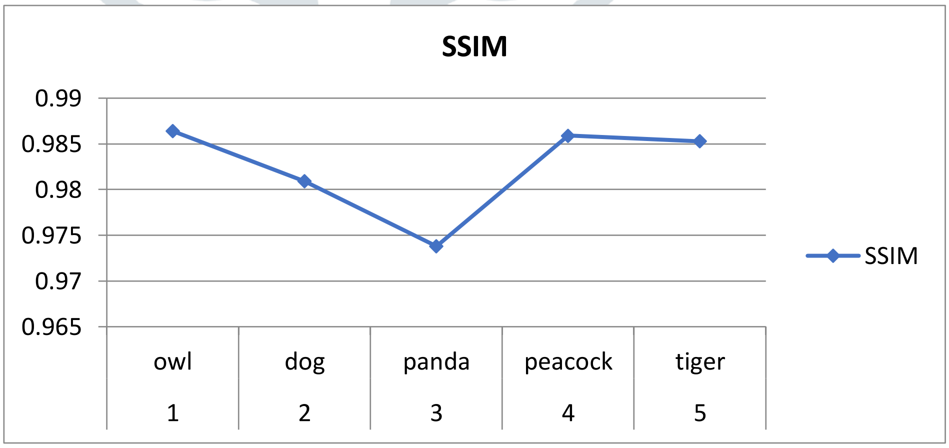

Fig 17.Experimental data of images with SSIM (Structural Similarity Index Measure) graph

.

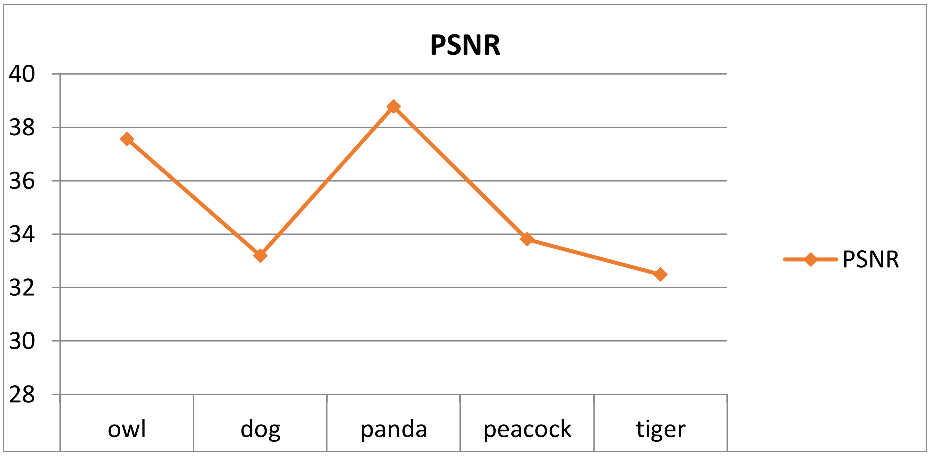

Fig 18. Experimental data of images with PSNR (Peak Signal-to-Noise Ratio) graph.

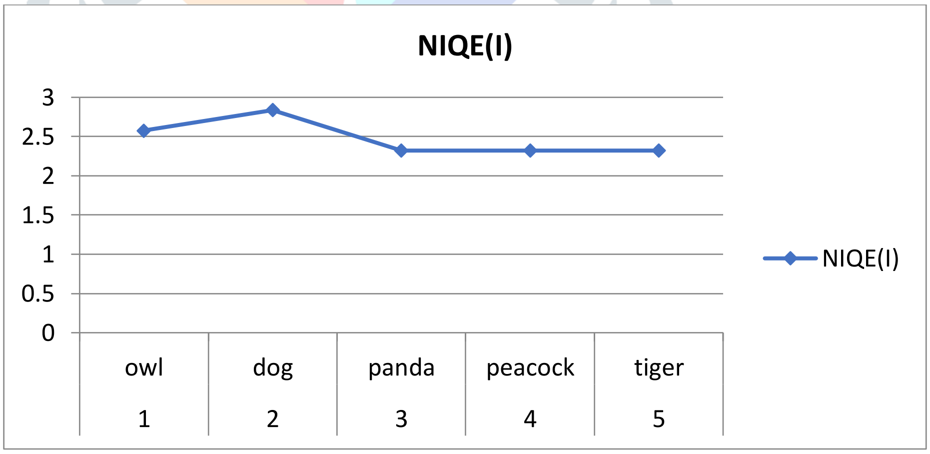

Fig 19. Experimental data of images with Naturalness Image Quality Evaluator (NIQE (I)) graph.

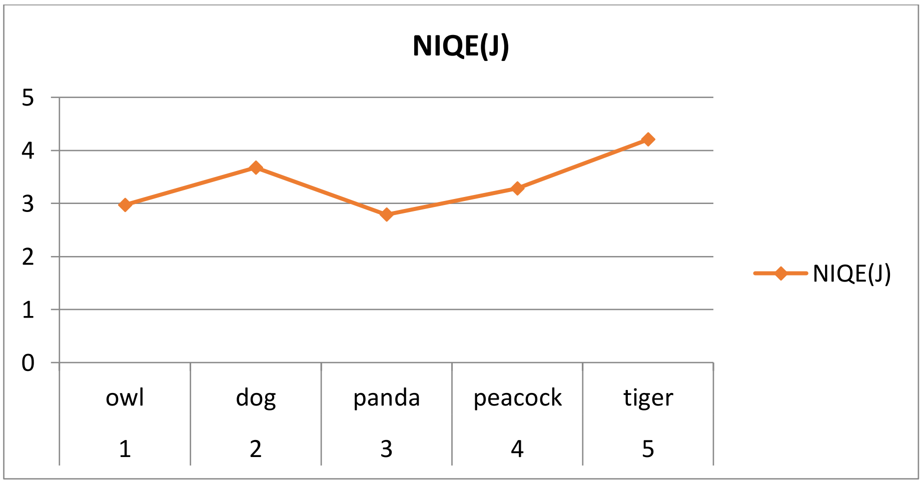

Fig 20. Experimental data of images with Naturalness Image Quality Evaluator (NIQE (J)) graph.

4. DISCUSSION

The *structural similarity index measure* or **SSIM** is a method to predict the perceived quality of any type of digital image or video. SSIM index is a full reference metric. It measures or predicts the image quality against the initial uncompressed or distortion-free image taken as the reference. It approaches to estimate the *absolute errors.* The *peak signal-to-noise ratio* or **PSNR** is a term used in image and signal processing as a quality measurement tool. PSNR of an image is obtained from the calculation of the logarithm of the *mean square error* (MSE), where MSE uses the summation method as its main component. The *naturalness image quality evaluator* or **NIQE.** Is a blind *image quality assessment* (IQA) tool used to measure thedeviations from the statistical regularities observed in the natural images, without training on human-rated distorted images. It extracts a set of local features from the image and fits those feature vectors to a multivariate Gaussian (MVG) model.

5. CONCUSTION

In this paper, we have presented the effect of the regularization parameter in a bilateral filter. SSIM, PSNR and NIQE are three functions in MATLAB which are used to determine the image quality or loss of quality with the encoding process of the filtered image to the original image. SSIM, PSNR and NIQE decreases with the increase. They both represent the human visual perception. The filter image or output image are seemed to be slightly blurred the edges become more sharpen and enhance the image, the filtered image becomes pleased to the human eyes. For better human visual perception, optimization is required. For that, more in-detailed work is under process in future work.

6. REFERENCES

[1] H. Halmaoui, A. Cord, and N. Hautiere, “Contrast restoration of road images taken in foggy weather,” in Proc. 2011 IEEE Int. Conf. Computer Vision Workshops, Barcelona, Spain, 2011, pp. 2057¡2063.

[2] S. Bronte, L. M. Bergasa, and P. F. Alcantarilla, “Fog detection system based on computer vision techniques,” in Proc. 12th Int. IEEE Conf. Intelligent Transportation Systems, St. Louis, MO, USA, 2009, pp. 1¡6.

[3] M. S. Shehata, J. Cai, W. M. Badawy, T. W. Burr, M. S. Pervez, R. J. Johannesson, and A. Radmanesh, “Video-based automatic incident detection for smart roads: The outdoor environmental challenges re-garding false alarms,” IEEE Trans. Intell. Transp. Syst., vol. 9, no. 2, pp. 349¡360, Jun. 2008.

[4] S. C. Huang, B. H. Chen, and Y. J. Cheng, “An efficient visibility enhancement algorithm for road scenes captured by intelligent trans-portation systems,” IEEE Trans. Intell. Transp. Syst., vol. 15, no. 5, pp. 2321¡2332, Oct. 2014.

[5] S. C. Huang, “An advanced motion detection algorithm with video quality analysis for video surveillance systems,” IEEE Trans. Circuits Syst. Video Technol., vol. 21, no. 1, pp. 1¡14, Jan. 2011.

[6] B. Xie, F. Guo, and Z. X. Cai, “Universal strategy for surveillance video defogging,” Opt. Eng., vol. 51, no. 10, pp. 101703, May2012.

[7] Z. Jia, H. C. Wang, R. E. Caballero, Z. Y. Xiong, J. W. Zhao, and A. Finn, “A two-step approach to see-through bad weather for surveillance video quality enhancement,” Mach. Vis. Appl., vol. 23, no. 6, pp. 1059¡1082, Nov. 2012.

[8] I. Yoon, S. Kim, D. Kim, M. H. Hayes, and J. Paik, “Adaptive defogging with color correction in the HSV color space for consumer surveillance system,” IEEE Trans. Consum. Electron., vol. 58, no. 1, pp. 111¡116, Feb. 2012.

[9] K. B. Gibson, D. T. Vo, and T. Q. Nguyen, “An investigation of dehazing effects on image and video coding,” IEEE Trans. Image Proc., vol. 21, no. 2, pp. 662¡673, Feb. 2012.

[10] M. Chacon-Murguia and S. Gonzalez-Duarte, “An adaptive neural-fuzzy approach for object detection in dynamic backgrounds for surveillance systems,” IEEE Trans. on Industr. Electron., vol. 59, no. 8, pp. 3286¡3298, Aug. 2012.

[11] S. Y. Tao, H. J. Feng, Z. H. Xu, and Q. Li, “Image degradation and recovery based on multiple scattering in remote sensing and bad weather condition,” Opt. Express, vol. 20, no. 15, pp. 16584¡16595, Jul. 2012.

[12] J. Long, Z. W. Shi, W. Tang, and C. S. Zhang, “Single remote sensing image dehazing,” IEEE Geosci. Remote Sens. Lett., vol. 11, no. 1, pp. 59¡63, Jan. 2014.

[13] A. Makarau, R. Richter, R. Muller, and P. Reinartz, “Haze detection and removal in remotely sensed multispectral imagery,” IEEE Trans. Geosci. Remote Sens., vol. 52, no. 9, pp. 5895¡5905, Sep. 2014.

[14] J. Liu, X. Wang, M. Chen, S. G. Liu, X. R. Zhou, Z. F. Shao, and P. Liu, “Thin cloud removal from single satellite images,” Opt. Express, vol. 22, no. 1, pp. 618¡632, Jan. 2014.

[15] H. F. Li, L. P. Zhang, and H. F. Shen, “A principal component based haze masking method for visible images,” IEEE Geosci. Remote Sens. Lett., vol. 11, no. 5, pp. 975¡979, May2014.

[16] X. X. Pan, F. Y. Xie, Z. G. Jiang, and J. H. Yin, “Haze removal for a single remote sensing image based on deformed haze imaging model,” IEEE Signal Process. Lett., vol. 22, no. 10, pp. 1806¡1810, Oct. 2015.

[17] L. X. Wang, W. X. Xie, and J. H. Pei, “Patch-based dark channel prior dehazing for RS multi-spectral image,” Chin. J. Electron., vol. 24, no. 3, pp. 573¡578, Jul. 2015.

[18] J. C. McCall and M. M. Trivedi, “Video-based lane estimation and tracking for driver assistance: Survey, system, and evaluation,” IEEE Trans. Intell. Transp. Syst., vol. 7, no. 1, pp. 20¡37, Mar. 2006. © 2022 JETIR May 2022, Volume 9, Issue 5 www.jetir.org (ISSN-2349-5162) JETIR2205108 Journal of Emerging Technologies and Innovative Research (JETIR) www.jetir.org b52

[19] J. P. Tarel, N. Hautiere, L. Caraffa, A. Cord, H. Halmaoui, and D. Gruyer, “Vision enhancement in homogeneous and heterogeneous fog,” IEEE Intell. Transp. Syst. Mag., vol. 4, no. 2, pp. 6¡20, Apr. 2012.

[20] M. Negru, S. Nedevschi, and R. I. Peter, “Exponential contrast restora-tion in fog conditions for driving assistance,” IEEE Trans. Intell. Transp. Syst., vol. 16, no. 4, pp. 2257¡2268, Aug. 2015.

[21] M. Pavlic, G. Rigoll, and S. Ilic, “Classification of images in fog and fog-free scenes for use in vehicles,” in Proc. 2013 IEEE Intelligent Vehicles Symposium, 2013, pp. 481¡486.
[22] N. Hautiere, J. P. Tarel, H. Halmaoui, R. Bremond, and D. Aubert, “En-hanced fog detection and free-space segmentation for car navigation,” Mach. Vis. Appl., vol. 25, no. 3, pp. 667¡679, Apr. 2014. [23] N. Hautiere, J. P. Tarel, and D. Aubert, “Mitigation of visibility loss for advanced camera-based driver assistance,” IEEE Trans. Intell. Transp. Syst., vol. 11, no. 2, pp. 474¡484, Jun. 2010.
[24] N. Hautiere, J. P. Tarel, and D. Aubert, “Towards fog-free in-vehicle vision systems through contrast restoration,” in Proc. 2007 IEEE Conf. Computer Vision and Pattern Recognition, Minneapolis, MN, USA, 2007, pp. 1¡8.
[25] H. J. Song, Y. Z. Chen, and Y. Y. Gao, “Velocity calculation by auto-matic camera calibration based on homogenous fog weather condition,” Int. J. Autom. Comput., vol. 10, no. 2, pp. 143¡156, Apr. 2013.
[26] R. Spinneker, C. Koch, S. B. Park, and J. J. Yoon, “Fast fog detection for camera based advanced driver assistance systems,” in Proc. IEEE 17th Int. Conf. Intelligent Transportation Systems, Qingdao, China, 2014, pp. 1369¡1374.
[27] R. Sato, K. Domany, D. Deguchi, Y. Mekada, I. Ide, H. Murase, and Y. Tamatsu, “Visibility estimation of traffic signals under rainy weather conditions for smart driving support,” in Proc. 15th Int. IEEE Conf. Intelligent Transportation Systems, Anchorage, AK, USA, 2012, pp. 1321¡1326.
[28] N. Carlevaris-Bianco, A. Mohan, and R. M. Eustice, “Initial results in underwater single image dehazing,” in Proc. 2010 IEEE OCEANS, Seattle, WA, USA, 2010, pp. 1¡8.
[29] C. Ancuti, C. O. Ancuti, T. Haber, and P. Bekaert, “Enhancing underwa-ter images and videos by fusion,” in Proc. 2012 IEEE Conf. Computer Vision and Pattern Recognition, Providence, RI, 2012, pp. 81¡88.
[30] J. Y. Chiang and Y. C. Chen, “Underwater image enhancement by wavelength compensation and dehazing,” IEEE Trans. Image Process., vol. 21, no. 4, pp. 1756¡1769, Apr. 2012.
[31] P. Drews, E. do Nascimento, F. Moraes, S. Botelho, and M. Campos, “Transmission estimation in underwater single images,” in Proc. 2013 IEEE Int. Conf. Computer Vision Workshops, Sydney, NSW, Australia, 2013, pp. 825¡830.
[32] H. M. Lu, Y. J. Li, and S. Serikawa, “Underwater image enhancement using guided trigonometric bilateral filter and fast automatic color cor-rection,” in Proc. 20th IEEE Int. Conf. Image Processing, Melbourne, VIC, Australia, 2013, pp. 3412¡3416.
[33] X. Y. Fu, P. X. Zhuang, Y. Huang, Y. H. Liao, X. P. Zhang, and X. H. Ding, “A retinex-based enhancing approach for single underwater image,” in Proc. 2014 IEEE Int. Conf. Image Processing, Paris, France, 2014, pp. 4572¡4576.
[34] S. H. Sun, S. P. Fan, and Y. C. F. Wang, “Exploiting image structural similarity for single image rain removal,” in Proc. 2014 IEEE Int. Conf. Image Processing, Paris, France, 2014, pp. 4482¡4486.
[35] S. D. You, R. T. Tan, R. Kawakami, and K. Ikeuchi, “Adherent raindrop detection and removal in video,” in Proc. 2013 IEEE Conf. Computer Vision and Pattern Recognition, Portland, OR, USA, 2013, pp. 1035¡1042.
[36] M. Desvignes and G. Molinie, “Raindrops size from video and image processing,” in Proc. 19th IEEE Int. Conf. Image Processing, Orlando, FL, USA, 2012, pp. 1341¡1344
[37] Z. Jia, H. C. Wang, R. Caballero, Z. Y. Xiong, J. W. Zhao, and A. Finn, “Real-time content adaptive contrast enhancement for see-through fog and rain,” in Proc. 2010 IEEE Int. Conf. Acoustics Speech and Signal Processing, Dallas, TX, USA, 2010, pp. 1378¡1381.
[38] K. Garg and S. K. Nayar, “When does a camera see rain?” in Proc. 10th IEEE Int. Conf. Computer Vision, Beijing, China, vol. 2, pp. 1067¡1074, 2005.
[39] H. Kawarabuki and K. Onoguchi, “Snowfall detection in a foggy scene,” in Proc. 22nd IEEE Int. Conf. Pattern Recognition, Stockholm, Sweden, 2014, pp. 877¡882.
[40] L. R. Bissonnette, “Imaging through fog and rain,” Opt. Eng., vol. 31, no. 5, pp. 1045¡1052, May1992.
[41] C. T. Cai, Q. Y. Zhang, and Y. H. Liang, “A survey of image dehazing approaches,” in Proc. 27th Chinese Control and Decision Conf., Qingdao, China, 2015, pp. 3964¡3969.
[42] Q. Wang and R. K. Ward, “Fast image/video contrast enhancement based on weighted thresholded histogram equalization,” IEEE Trans. Consum. Electron., vol. 53, no. 2, pp. 757¡764, May2007.
[43] R. Dale-Jones and T. Tjahjadi, “A study and modification of the local histogram equalization algorithm,” Pattern Recogn., vol. 26, no. 9, pp. 1373¡1381, Sep. 1993.
[44] M. F. Khan, E. Khan, and Z. A. Abbasi, “Segment dependent dynamic multi-histogram equalization for image contrast enhancement,” Digit. Signal Process., vol. 25, pp. 198¡223, Feb. 2014.
[45] T. Celik and T. Tjahjadi, “Contextual and variational contrast enhance-ment,” IEEE Trans. Image Process., vol. 20, no. 12, pp. 3431¡3441, Dec. 2011.
[46] T. K. Kim, J. K. Paik, and B. S. Kang, “Contrast enhancement system using spatially adaptive histogram equalization with temporal filtering,” IEEE Trans. Consum. Electron. vol. 44, no. 1, pp. 82¡87, Feb. 1998. © 2022 JETIR May 2022, Volume 9, Issue 5 www.jetir.org (ISSN-2349-5162) JETIR2205108 Journal of Emerging Technologies and Innovative Research (JETIR) www.jetir.org b53
[47] J. Y. Kim, L. S. Kim, and S. H. Hwang, “An advanced contrast enhance-ment using partially overlapped sub-block histogram equalization,” IEEE Trans. Circuits Syst. Video Technol., vol. 11, no. 4, pp. 475¡484, Apr. 2001.
[48] S. C. Huang and C. H. Yeh, “Image contrast enhancement for preserv-ing mean brightness without losing image features,” Eng. Appl. Artif. Intell., vol. 26, no. 5¡6, pp. 1487¡1492, May¡Jun. 2013.
[49] H. T. Xu, G. T. Zhai, X. L. Wu, and X. K. Yang, “Generalized equalization model for image enhancement,” IEEE Trans. Multimed., vol. 16, no. 1, pp. 68¡82, Jan. 2014.
[50] Wang, Wencheng & Yuan, Xiaohui. (2017). Recent advances in image dehazing. IEEE/CAA Journal of Automatica Sinica. 4. 410-436. 10.1109/JAS.2017.7510532.
[51] S Roy, S S Chaudhuri, Cuckoo search algorithm using Lévy flight: a review, IJMECS, vol-5(12), December 2013.
[52] S Roy, S Biswas, S S Chaudhuri, Nature-inspired swarm intelligence and its applications, IJMECS, vol-6(12), December 2014.
[53] S Roy, S S Chaudhuri, Error Measurement & its Impact on Bilateral - Canny Edge Detector-A Hybrid Filter, IJMECS, vol-8(2), February 2016
[54] S Roy, S S Chaudhuri, Modeling of Haze image as Ill-posed inverse problem & its solution, IJMECS, vol-8(12), 2016.
[55] S Roy, S S Chaudhuri, WLMS-based Transmission Refined Self-Adjusted No Reference Weather Independent Image Visibility Improvement, IETE Journal of Research, September 2019.
[56] K. He, J. Sun, X. Tang, “Image Guided Filtering”, *IEEE Transactions on Pattern Analysis & Machine Intelligence*, VOL. 35 No. 10

[57] Gonzalez, R. C. and Woods, R. E. [2008]. *Digital Image Processing*, 3rd ed., Prentice Hall, Upper Saddle River, NJ
[58] K. He, J. Sun, X. Tang, "Image Guided Filtering", *Proc. European Conf. Computer Vision*, pp. 1-14, 2010.
[59] N. Draper and H. Smith, *Applied Regression Analysis*, 3rd ed. John Wiley, 1981.
[60] T. Hastie, R. Tibshirani, and J.H. Friedman, *The Elements of Statistical Learning*. 2nd ed. Springer, 2003.
[61] S. Roy, S. Chaudhuri, "WLMS-based Transmission Refined Self-Adjusted No Reference Weather Independent Image Visibility Improvement", *IETE Journal of Research*, 2019
[62] A Nilam, S Roy, Image Dehazing Advancement, Journal of Emerging Technologies and Innovative Research (JETIR),V-9 (5), pp-(b45-b53), ISSN-2349-5162.

Author Details:-

Sourav Dutta

sdutta079@gmail.com

Sourav Dutta completed Diploma in Electronics and Communication Engineering,Bangalore after he completed B.tech in Electronics and Communication Engineering from Narula Institute of Technology,kolkata and currently he is perusing M.tech from Electronics and Communication Engineering from Narula Institute Of Technology, Kolkata.

Arpita Santra

arpita.santra@nit.ac.in

Arpita Santra has completed B.Tech and M.Tech in Electronics and Communication Engineering from Kalyani Govt. Engg. College, Kalyani, West Bengal, India. Currently she is working as Assistant Professor, Dept. of ECE at Narula Institute of Technology, Kolkata. Her research interests are Microwave Sources and Micro strip Antenna Design.

Dr. Sangita Roy

roysangita@gmail.com

Sangita Roy is an Associate Professor at ECE Department, Narula Institute of Technology. She has a teaching experience of more than 24 years. She was in Bells Controls Limited (industry) for two years and West Bengal State Centre, IEI (Kolkata) in administration for two years. She completed her Diploma (ETCE), A.M.I.E (ECE) and M-Tech (Comm. Egg.), Ph.D. (Computer Vision) at ETCE Department of Jadavpur University. She is member of IETE, FOSET, ISOC, IEEE ComSoc, and IEEE CAS. She has published numerous journals, book chapters and conference papers. Scholars are working under her guidance in Computer Vision, Image processing and ML, AI.